Atmospheric and Oceanic Science Letters

ISSN: 1674-2834 (Print) 2376-6123 (Online) Journal homepage: http://www.tandfonline.com/loi/taos20

Anomalous pattern of ocean heat content during different phases of the solar cycle in the tropical Pacific

Wen-Juan HUO & Zi-Niu XIAO

To cite this article: Wen-Juan HUO & Zi-Niu XIAO (2017) Anomalous pattern of ocean heat content during different phases of the solar cycle in the tropical Pacific, Atmospheric and Oceanic Science Letters, 10:1, 9-16, DOI: 10.1080/16742834.2017.1247412

To link to this article: http://dx.doi.org/10.1080/16742834.2017.1247412

Accepted author version posted online: 12 Oct 2016.
Published online: 27 Oct 2016.

ATMOSPHERIC AND OCEANIC SCIENCE LETTERS, 2017
VOL. 10, NO. 1, 9–16
http://dx.doi.org/10.1080/16742834.2017.1247412

Taylor & Francis
Taylor & Francis Group

Anomalous pattern of ocean heat content during different phases of the solar cycle in the tropical Pacific

HUO Wen-Juan[a,b] and XIAO Zi-Niu[a]

[a]State Key Laboratory of Numerical Modeling for Atmospheric Sciences and Geophysical Fluid Dynamics, Institute of Atmospheric Physics, Chinese Academy of Sciences, Beijing, China; [b]College of Earth Science, University of Chinese Academy of Sciences, Beijing, China

ABSTRACT

Solar radiation is a forcing of the climate system with a quasi-11-year period. As a quasi-period forcing, the influence of the phase of the solar cycle on the ocean system is an interesting topic of study. In this paper, the authors investigate a particular feature, the ocean heat content (OHC) anomaly, in different phases of the total solar irradiance (TSI) cycle. The results show that almost opposite spatial patterns appear in the tropical Pacific during the ascending and declining phases of the TSI cycle. Further analysis reveals the presence of the quasi-decadal (~11-year) solar signal in the SST, OHC and surface zonal wind anomaly field over the tropical Pacific with a high level of statistical confidence (>95%). It is noted that the maximum centers of the ocean temperature anomaly are trapped in the upper ocean above the main pycnocline, in which the variations of OHC are related closely with zonal wind and ocean currents.

摘要

具有准11年周期的太阳辐射是地球气候系统的主要能量来源。作为一个准周期强迫，太阳辐射周期变化的位相对热带太平洋海洋热状态的影响值得关注。本文中，作者分析了在太阳总辐射不同位相下，热带太平洋海洋热含量的异常特征。结果表明在太阳活动的上升位相和下降位相，海洋热含量异常的空间型几乎是对称的，而异常值则是相反的。进一步分析表明，在热带太平洋的某些区域，在海洋表面温度，海洋热含量和表面风场中均存在显著的准11年太阳信号。海洋温度异常的最大值中心位于主温跃层以上的次表层。不同太阳位相之间热含量异常的转变与表面纬向风异常以及热带太平洋地区的洋流密切相关。

ARTICLE HISTORY
Received 31 March 2016
Revised 27 June 2016
Accepted 10 August 2016

KEYWORDS
Ocean heat content anomaly; total solar irradiance; solar cycle; tropical Pacific

关键词
海洋热含量; 太阳总辐射; 太阳活动; 热带太平洋

1. Introduction

Total solar irradiance (TSI), as the most common indicator of solar radiation, is a forcing of the earth–climate system with a quasi-11-year period. However, its variation is very small (about 0.1%), so the net thermal forcing of the climate system can be ignored (Foukal et al. 2006). Nonetheless, in many previous studies, the decadal-scale solar signal has been detected in the troposphere and ocean, especially in the tropical Indo-Pacific region. Meehl and Arblaster (2009) revealed that a La Niña-like SST anomaly pattern response appears in peak years of the TSI cycle, followed by an El-Niño-like response after one or two years, over the tropical Pacific. Its corresponding mechanisms are cited as 'top-down' and 'bottom-up' amplification mechanisms. Meanwhile, Tung and Zhou (2010) and Roy (2014) found that it is not a La Niña-like or El Niño-like response in the tropical central eastern Pacific, but a weak warming in the SST at solar maximum compared with that at solar minimum. In Misios and Schmidt (2012), the ensemble simulations from an AOGCM showed that the tropical SST oscillates almost in-phase with the 11-year solar cycle. White and Liu (2008) also found the fluctuation of the upper ocean warming to be in-phase with TSI on the decadal scale during the twentieth century, governed by a resonant excitation of the tropical delay action oscillator and solar forcing, and the warming stage lagged the solar peak year by one to three years.

Therefore, from previous studies, there is consensus over the existence of the quasi-decadal solar signal (~11 years) in the tropical Pacific, but conclusions regarding the responses to that signal remain under debate. Friis-Christensen and Lassen (1991) were the first to use the length of the solar cycle as an indicator of solar activity to find its relationship with surface temperature. Then, Stauning (2011), using the cycle-average sunspot number to represent solar activity, found in-cycle variations

CONTACT XIAO Zi-Niu xiaozn@lasg.iap.ac.cn

of global temperature corresponded to the TSI level. Recently, Maliniemi, Asikainen, and Mursula (2014) found that Northern Hemispheric winter temperature anomaly patterns are significantly different during the different phases (minimum, ascending, maximum, and declining) of the solar cycle. Under TSI variation as a quasi-decadal forcing, when its intensity steps up (down), the affected system would attain a new steady state after a period of time (Stauning 2011).

The ocean, as a major component of the climate system, plays a crucial role in regulating Earth's climate. The ocean heat content (OHC) anomaly always lags behind the forcing change due to its immense thermal inertia. So, in this study, considering the equilibration timescales of OHC and its hysteretic response to the solar peak (White et al. 1997), we focus on the phases of the solar cycle to detect the ocean thermal state anomaly.

Following this introduction, in Section 2, we describe the data and method used in this study. In Section 3 we present the results regarding the phases of the TSI cycle, the OHC and potential temperature anomaly during different phases, and solar signal detection. Section 4 further discusses the responses in the ocean thermal state to solar forcing and its corresponding dynamic environment anomaly. Finally, concluding remarks are provided in Section 5.

2. Data and method

TSI is calculated by integrating the entire spectrum of solar energy flux arriving at the top of the terrestrial atmosphere at mean Sun–Earth distance. This was used as an index of the level of solar radiation in this study. Historical TSI reconstruction from 1610 to 2015 was obtained from the University of Colorado at Boulder Solar Radiation & Climate Experiment (SORCE) (http://lasp.colorado.edu/home/sorce/files/2011/09/TSI_TIM_Reconstruction.txt).

In this study, we used the OHC anomaly and ocean potential temperature anomaly as parameters of the ocean thermal state. The OHC anomaly fields for depths of 0–700 m were provided by the NOAA, National Center for Environmental Information, available at: http://www.nodc.noaa.gov/OC5/3M_HEAT_CONTENT/. These monthly data spanned from January 1955 to January 2016. The ocean potential temperature was obtained from the Met Office Hadley Centre datasets of global quality-controlled ocean temperature and salinity profiles and objective analyses. Here, we used the objective analyses in the newest version, EN.4.1.1, which was available from 1900 to February 2016 (http://hadobs.metoffice.com/en4/).

Additionally, a number of surface data types, such as SST and zonal wind (0.995 sigma level), were used for further analysis. These data were provided by NOAA/OAR/ESRL PSD, Boulder, Colorado, USA.

Power spectrum analysis is a common method used to extract potential periodic components. We used this method to detect the solar cycle signal in the ocean thermal state and zonal wind.

As we know, the ENSO signal is very strong in the tropical Pacific; thus, a seven-year low-pass filter with Cornelius Lanczos filter weights (Duchon 1979) was used to remove fluctuations of less than seven years. In this study, all data were detrended before statistical analysis, and anomalies were defined as the departure from the annual mean or seasonal average. Data used for composite analysis had already been seven-year low-pass filtered. Considering the time periods for valid data, we used data for the period 1955–2015.

3. Results

3.1. Phases of the TSI cycle in OHC

Previous studies have noted the variations in the direct absorption of TSI by oceans. This is because oceans have a large heat capacity, which can 'integrate' long-term, small variations in heat input (Gray et al. 2010). From this perspective, the variations of TSI may have some impact on ocean heat storage in the tropical Pacific. The geographical distributions of correlation coefficients between TSI and the OHC anomaly at time lags of 0, 1, 2 and 3 years are given in Figure 1. The results demonstrate an obvious pattern, with positive correlation in the tropical central and eastern Pacific but negative in the west. When OHC lags TSI by two years, the confidence level in some regions of the tropical Pacific is beyond 95% (black dotted regions within black contours in Figure 1).

Although the mechanisms are not yet clear, OHC anomaly is sensitive to variation of solar radiance in some regions of the tropical Pacific. And the maximum response of the ocean heat storage anomaly occurs for the two-year lag, which may be due to the ocean thermal inertia (White et al. 1997; White and Liu 2008). Solar radiation is a gradually changing forcing with quasi-periodicity, and its accumulation and persistent effect may depend on its phases. Therefore, in this study, we focus on the phases of the TSI cycle to detect the thermal state anomaly in the tropical Pacific.

The phases of the TSI cycle are defined as a function of TSI values. Considering the asymmetry and difference in amplitude and length of every TSI cycle, each TSI cycle is normalized independently. An ascending phase is defined as the period from the valley year to the year previous to the solar peak, and a declining phase is defined as the period from the peak year to the year previous to the solar valley.

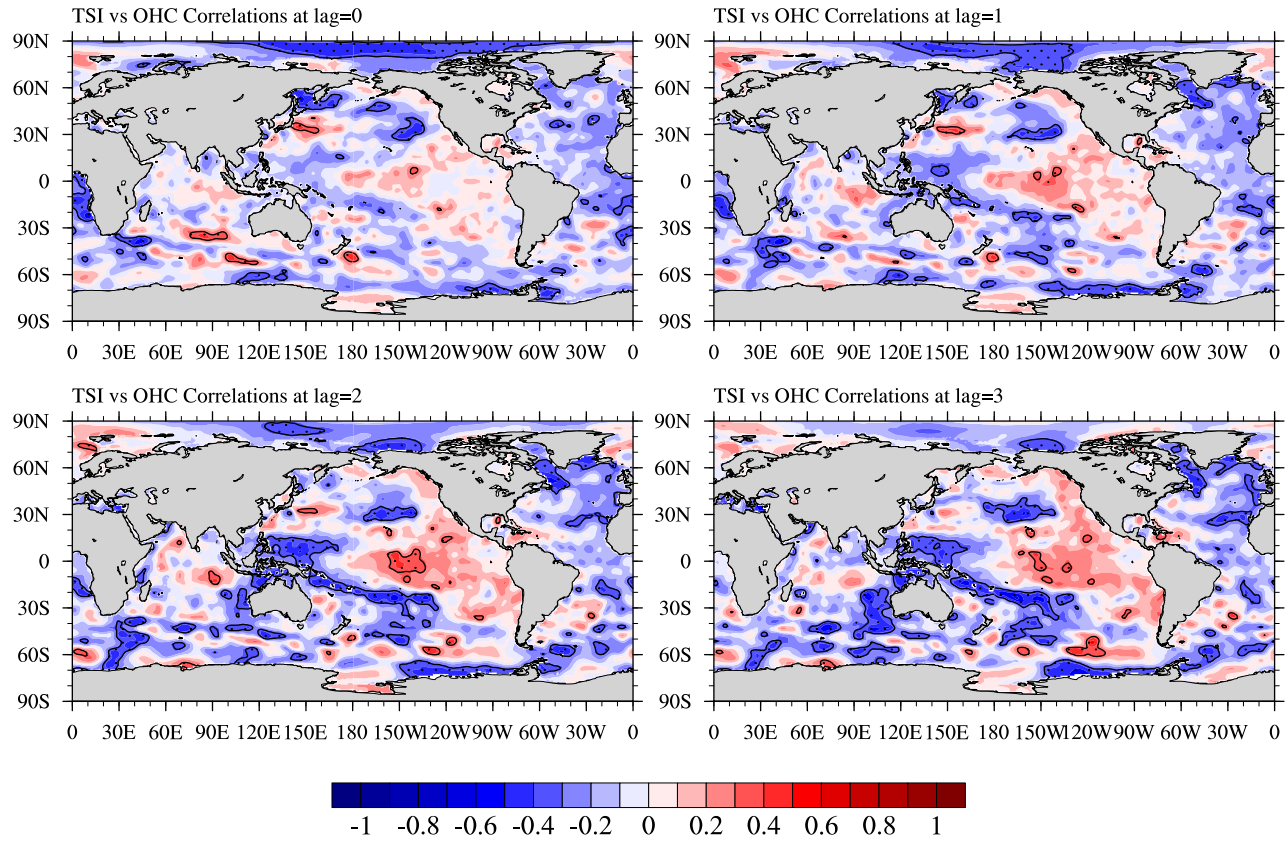

Figure 1. Geographical distribution of correlation coefficients between TSI and the OHC anomaly at time lags of 0, 1, 2, and 3 years.
Note: Black dotted regions within black contours are above the 95% confidence level.

Each of the phases is divided into four stages with almost equal sample sizes, as shown in Figure 2 (upper panel). The ascending phase includes four stages: A, valley stage (0–0.1); B, initial ascending stage (0.1–0.4); C, intermediate ascending stage (0.4–0.6); D, last ascending stage (0.6–0.9). And there are also four stages in the declining phase: E, peak stage (1–0.9); F, initial declining stage (0.9–0.6); G, intermediate declining stage (0.6–0.4); H, last declining stage (0.4–0.1). The years involved in each phase for this study are shown in Table 1.

3.2. OHC and potential temperature anomalies during different phases of the TSI cycle in the tropic Pacific

In order to investigate the OHC features during different phases of TSI, composites of the OHC anomaly during the ascending and declining phases of the TSI cycle are given in Figure 3. As shown in Figure 3, during the ascending phases of the TSI cycle (top panel), the OHC displays a positive anomaly center in the tropical western Pacific but a negative anomaly center in the central Pacific (dotted shaded regions are beyond the 95% confidence level), while a weak negative OHC anomaly is apparent in the eastern Pacific. On the other hand, the anomaly pattern is the opposite during the declining phase (bottom panel). The results demonstrate a negative anomaly in the tropical western Pacific but a positive anomaly in the central and eastern Pacific.

The different features during the ascending and declining phases of the TSI cycle are also found in the subsurface ocean temperature field. The composite potential temperature anomaly along the longitude averaged in the equatorial Pacific (10°S–10°N) from the surface to a depth of 300 m during different phases of the TSI cycle is shown in Figure 4. During the ascending phase of the TSI cycle (Figure 4(a)), a clear positive potential temperature anomaly appears in the tropical western Pacific, while a negative anomaly is situated in the central and eastern Pacific. This feature is opposite during the declining phase (Figure 4(b)), which is consistent with the OHC anomaly characteristics revealed in Figure 3.

3.3. Solar signals in the tropical Pacific

As reported above, it was found that the ocean thermal average state in the tropical Pacific is almost opposite during the ascending and declining phases of the TSI cycle. This means that the ocean heat storage anomaly is phase-locked on average with the phases of the

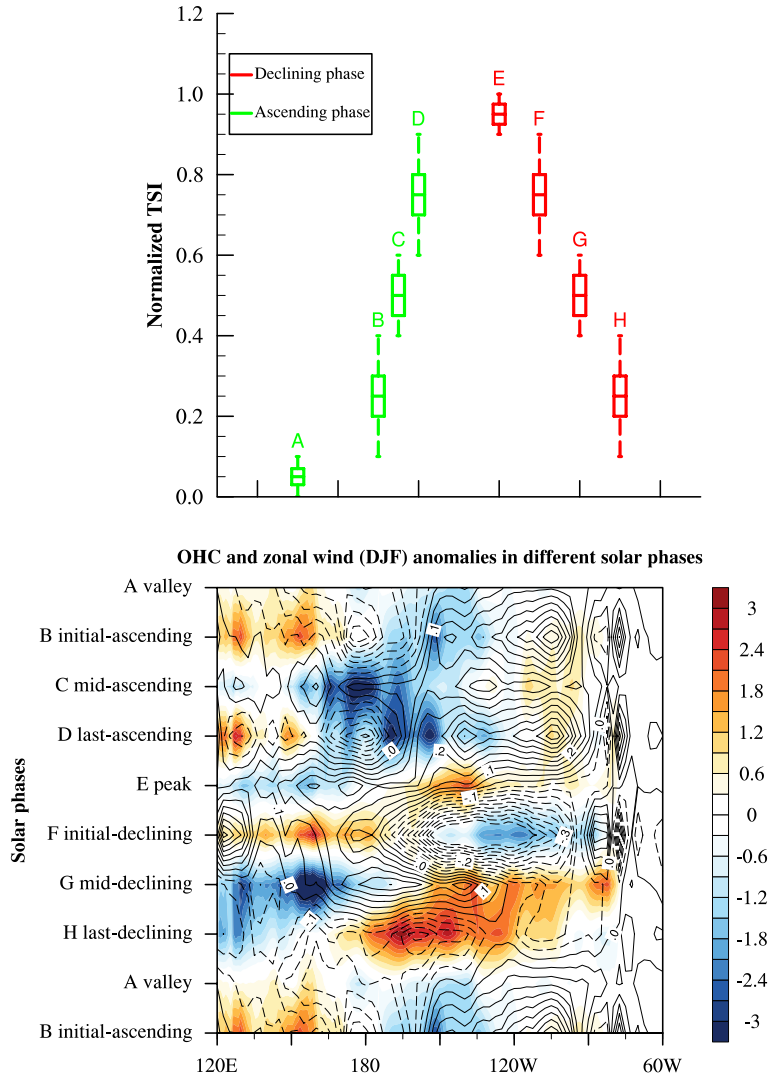

Figure 2. Upper panel: Conceptual sketch for the phases of the TSI cycle. Lower panel: Stage–longitude diagram of the composite OHC anomaly (color shading) overlaid with the zonal wind anomaly (December–February) (contour lines) averaged in the tropical Pacific (15°S–15°N) during different phases.
Notes: The ascending phase includes: A, valley; B, initial-ascending; C, intermediate-ascending; D, last-ascending. The declining phase includes: E, peak; F, initial-declining; G, intermediate-declining; H, last-declining.

Table 1. Years involved in each phase of the TSI cycle.

Solar phase	Years
Ascending	1955–57, 1964–67, 1975–78, 1984–88, 1996–99, 2007–11
Declining	1958–63, 1968–74, 1979–83, 1989–95, 2000–06, 2012–15

TSI cycle. If this is true, they should have similar characteristics of variation. Power spectrum analysis was employed to confirm this assumption. We took some significant OHC anomaly regions in the tropical Pacific as 'solar-sensitive' regions, as shown by the boxes in Figure 3. Area_W (10°N–15°S, 120°–160°E) and Area_E (10°N–15°S, 160°–120°W) are taken for OHC (black boxes in Figure 3) analysis, while Area_A (10°S–10°N, 160°E–130°W) and Area_M (5°N–5°S, 160°E–160°W) are taken for SST (white box in Figure 3) and zonal wind (red box in Figure 3) analysis, respectively.

The periodic characteristics of OHC, SST and zonal wind anomaly variation are shown in Figure 5. The quasi-11-year period of OHC in Area_W and Area_E is noticeable in Figure 5(a) and (b), although it is somewhat weak compared to the 2–7-year period, which should present the ENSO cycle. After low-pass filtering with Lanczos filter weights (Duchon 1979) to remove fluctuations less than 7 years, the quasi-11-year period becomes the dominant period, as shown in Figure 5(c) and (d). The power spectrum of the SST anomaly demonstrates two principal periods of 11 years and 3.7 years (>95% confidence level) in Area_A in Figure 5(e). And two prominent periods of 11 years and 2.5 years (>95% confidence level) are apparent for the zonal wind anomaly in Area_M (Figure 5(f)). These results illustrate the possibility that these sensitive regions contain a quasi-11-year solar signal.

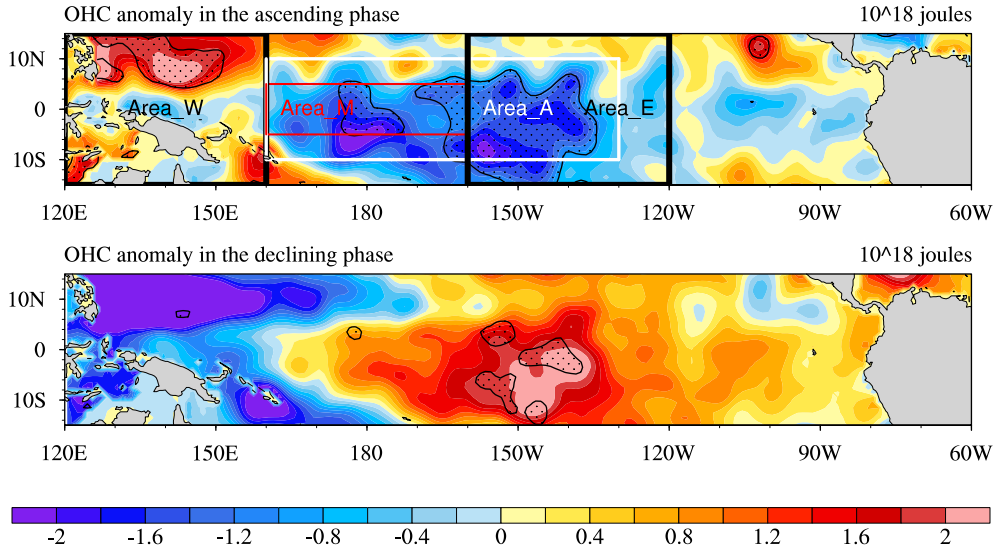

Figure 3. Composite OHC anomalies during the ascending phase (top) and declining phase (bottom) of the TSI cycle.
Note: Dotted shaded regions represent the confidence level above 95% (Student's *t*-test).

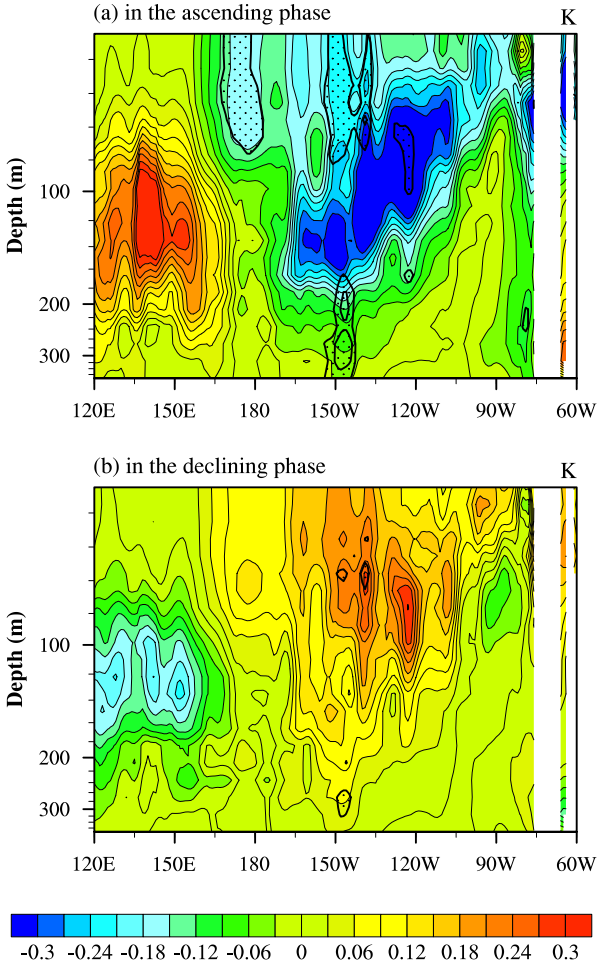

Figure 4. Composite potential temperature anomaly along the longitude averaged in the equatorial Pacific (10°S–10°N) during the ascending phase (top) and declining phase (bottom) of the TSI cycle.
Note: Dotted shaded regions represent the confidence level above 95% (Student's *t*-test).

Through the above analysis, a noticeable quasi-decadal solar signal (~11 years) does indeed exist in the OHC, SST, and surface zonal wind anomaly fields in some regions of the tropical Pacific, with a high level of statistical significance (>95%). However, the spatial pattern of the OHC anomaly is almost opposite in different phases of the TSI cycle. A possible reason for this might depend on the cloud distribution over the tropical Pacific. As we know, the cloud fraction reaches a minimum in the tropical eastern Pacific, and this clear sky condition means more solar radiation reaches the surface. The surface warm water heated by the Sun's radiation in these cloud-free areas is transported westward by the ocean surface currents. With solar radiation increasing, the meridional temperature gradient in the tropical Pacific is decreased. In the declining phase, when the solar radiation reaches its maximum, westerly wind anomalies in the western equatorial Pacific would reduce the westward transportation, and more warm water would accumulate in the central and eastern Pacific. As a result, the state of the OHC anomaly would change into a positive anomaly in the central and eastern Pacific.

4. Discussion

From the above composite analysis, the features of the ocean thermal anomaly are spatially symmetric patterns depending on different solar cycle phases. In order to further understand the connections between solar activity and OHC anomaly patterns, we divide each phase into four stages, as shown in Figure 2.

Stage–longitude cross section of the composite OHC anomaly overlaid with the zonal wind anomaly averaged in the tropical Pacific (15°S–15°N) is shown in Figure 2.

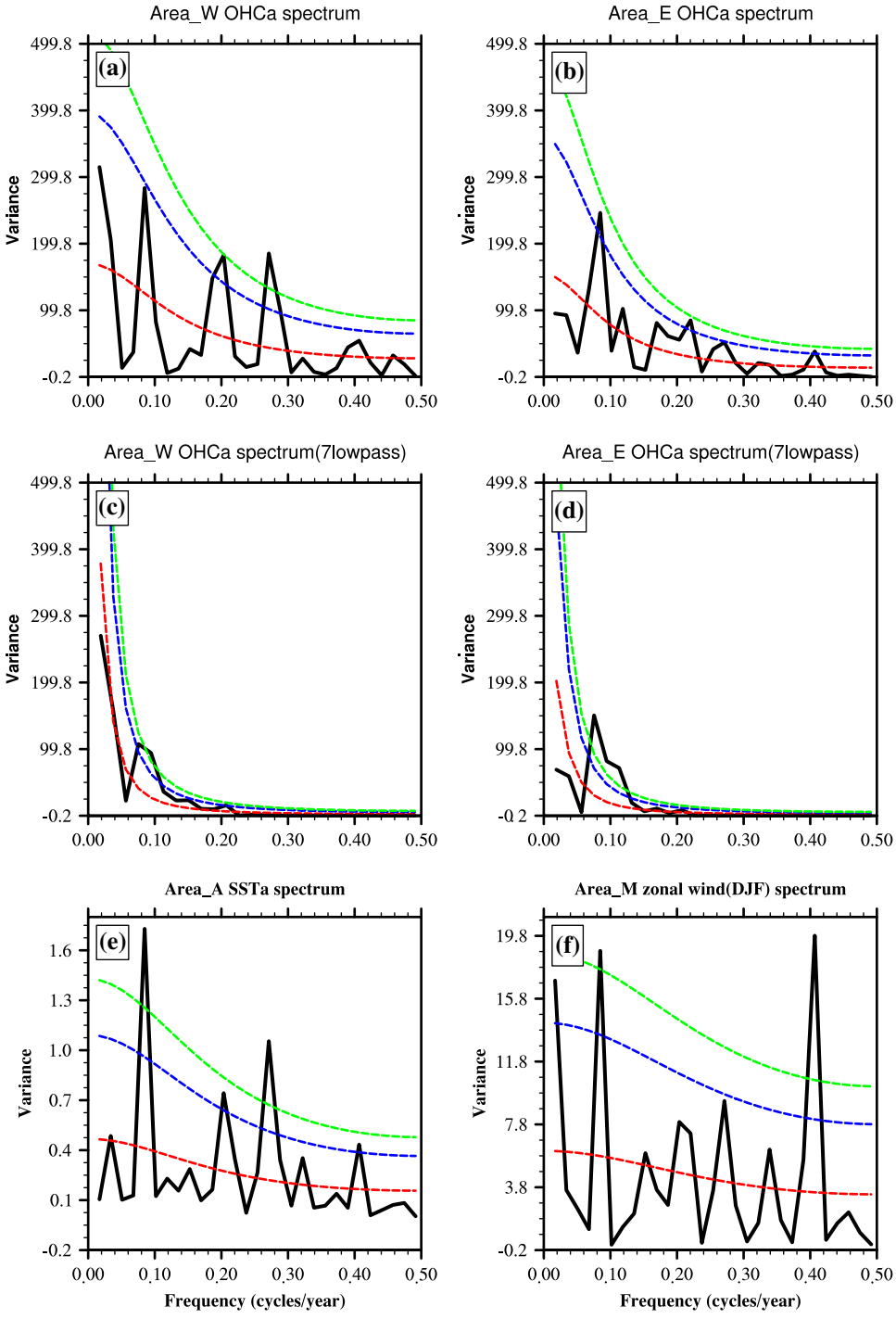

Figure 5. Power spectra of the OHC anomaly in (a) Area_W and (b) Area_E in the raw data. Power spectra of the OHC anomaly after seven year low-pass filtering in (c) Area_W and (d) Area_E, with explained variances of 58.47% and 65.94%, respectively. (e) Power spectrum of the SST anomaly in Area_A. (f) Power spectrum of the zonal wind (December–February) in Area_M.
Note: The red dashed line represents theoretical red noise spectrum, with confidence levels represented by the blue dashed line (90%) and green dashed line (95%).

During the first stage (A) in the ascending phase, a positive OHC anomaly appears in the tropical western Pacific but a negative anomaly is situated in the central and eastern Pacific. In the following stages, the negative anomaly propagates westward. A positive anomaly signal appears and enlarges in the eastern Pacific. In this process, the SSH in the western Pacific is higher than in the central and eastern Pacific, meaning the equatorial undercurrent will increase in the central Pacific (Drenkard and Karnauskas 2014). The positive anomalous subsurface water is transported from west to east in the tropical Pacific along the thermocline and results in upwelling in the eastern boundary of the

Pacific. In the meantime, anomalous westerlies cover the tropical eastern Pacific during the whole ascending phase, which suppresses the upwelling there, and a weak positive anomaly presents in the eastern Pacific (east of 120°W). The anomalous easterlies are noticeable in the central Pacific, which induce the OHC negative anomaly center to move westward.

However, at the same time, more solar radiation heats the ocean water directly over the cloud-free area until the solar forcing climbs to its maximum peak. In the peak stage (E), a significant OHC positive anomaly appears in the central and eastern tropical Pacific, and this positive anomaly increases in the next two declining stages (G and H) while a negative anomaly occurs in the western Pacific. During the declining phase, the quasi-equilibrium thermal state of the tropical Pacific (positive-west and negative-east) is broken in the peak stage by a positive anomaly in the central and eastern Pacific, and ultimately results in a new quasi-equilibrium state (negative-west and positive-east).

After the peak stage (E), a stronger solar heating effect in the cloud-free areas would reduce the meridional temperature gradient in the tropical Pacific. Anomalous westerlies occur in the tropical western Pacific, and zonal wind convergence in the central equatorial Pacific makes more warm water accumulate there and sink into the subsurface, which deepens the thermocline and decreases the speed of the equatorial undercurrent. As a result, the positive OHC anomaly in the central and eastern Pacific enhances during the declining phase. When anomalous easterlies prevail in the central Pacific (H in Figure 2), a stronger positive OHC anomaly extends to the west.

Clearly, there is a negative OHC anomaly in the eastern Pacific but a positive OHC anomaly in the western Pacific during the initial declining stage (F), which may be a result of the strong La Niña event in 1973/1974 (Shabbar and Yu 2009).

Based on the above analysis, the variation of TSI may directly affect the ocean heat storage in cloud-free areas. However, due to the strong air–sea interaction in the tropics, the temperature anomaly would induce anomalies in corresponding dynamic parameters, such as zonal wind and ocean currents, and those dynamic anomalies then regulate the geographical distribution of the thermal anomaly.

5. Conclusion

As commonly known, solar radiation is a periodic external forcing with a quasi-11-year cycle. It is reasonable to assume that the response of the climate system to this forcing will result in different climatic states in different phases. In this study, we investigated the OHC anomaly pattern during different phases of the TSI cycle. The results showed that the patterns of OHC and potential temperature anomalies in the tropical Pacific are quite spatially symmetric in the ascending and declining phases, which seems phase-locked with the phases of the TSI cycle. The most significant regions of the OHC anomaly are locate just in the high correlation areas (beyond the 95% confidence level), which are 'solar-sensitive' regions with a clear quasi-11-year period.

Further analysis on the OHC anomaly patterns revealed that its phase-locked feature is related with air–ocean interaction. Solar radiation warms the ocean water and increases the heat storage in cloud-free areas. On the other hand, the thermal anomaly changes surface zonal wind and ocean undercurrents. Ultimately, it regulates and amplifies the OHC anomaly. However, the process and amplitude of the ocean heat storage anomaly response to solar forcing remains under debate; the possible mechanisms need to be investigated further in future.

Disclosure statement

No potential conflict of interest was reported by the authors.

Funding

This work was supported by the National Basic Research Program of China [grant number 2012CB957804]; the External Cooperation Program of Bureau of International Co-operation, Chinese Academy of Sciences [grant number 134111KYSB20150016].

References

Drenkard, E. J., and K. B. Karnauskas. 2014. "Strengthening of the Pacific Equatorial Undercurrent in the SODA Reanalysis: Mechanisms, Ocean Dynamics, and Implications." *Journal of Climate* 27: 2405–2416. doi:10.1175/JCLI-D-13-00359.1.

Duchon, C. E. 1979. "Lanczos Filtering in One and Two Dimensions." *Journal of Applied Meteorology* 18: 1016–1022. doi:10.1175/1520-0450(1979)018<1016:LFIOAT>2.0.CO;2.

Foukal, P., C. Fröhlich, H. Spruit, and T. M. L. Wigley. 2006. "Variations in Solar Luminosity and Their Effect on the Earth's Climate." *Nature* 443: 161–166. doi:10.1038/nature05072.

Friis-Christensen, E., and K. Lassen. 1991. "Length of the Solar Cycle: An Indicator of Solar Activity Closely Associated with Climate." *Science* 254: 698–700. doi:10.1126/science.254.5032.698.

Gray, L. J., J. Beer, M. Geller, J. D. Haigh, M. Lockwood, K. Matthes, and U. Cubasch. 2010. "Solar Influences on Climate." *Reviews of Geophysics* 48: RG4001. doi:10.1029/2009RG000282.

Maliniemi, V., T. Asikainen, and K. Mursula. 2014. "Spatial Distribution of Northern Hemisphere Winter Temperatures during Different Phases of the Solar Cycle." *Journal of Geophysical Research: Atmospheres* 119: 9752–9764. doi:10.1002/2013JD021343.

Meehl, G. A., and J. M. Arblaster. 2009. "A Lagged Warm Event-like Response to Peaks in Solar Forcing in the Pacific Region." *Journal of Climate* 22: 3647–3660. doi:10.1175/2009JCLI2619.1.

Misios, S., and H. Schmidt. 2012. "Mechanisms Involved in the Amplification of the 11-Yr Solar Cycle Signal in the Tropic Pacific Ocean." *Journal of Climate* 25: 5102–5118. doi:10.1175/JCLI-D-11-00261.1.

Roy, I. 2014. "The Role of the Sun in Atmosphere-ocean Coupling." *International Journal of Climate* 34: 655–677. doi:10.1002/joc.3713.

Shabbar, A., and B. Yu. 2009. "The 1998-2000 La Nina in the Context of Historically Strong La Niña Events." *Journal of Geophysical Research* 114: D13105. doi:10.1029/2008JD011185.

Stauning, P. 2011. "Solar Activity-climate Relations: A Different Approach." *Journal of Atmospheric and Solar-terrestrial Physics* 73 (2011): 1999–2012. doi:10.1016/j.jastp.2011.06.011.

Tung, K.-K., and J. Zhou. 2010. "The Pacific's Response to Surface Heating in 130 yr of SST: La Niña-like or El Niño-like?" *Journal of the Atmospheric Sciences* 67: 2649–2657. doi:10.1175/2010JAS3510.1.

White, W. B., and Z. Liu. 2008. "Resonant Excitation of the Quasi-decadal Oscillation by the 11-Year Signal in the Sun's Irradiance." *Journal of Geophysical Research* 113: C01002. doi:10.1029/2006JC004057.

White, W. B., J. Lean, D. R. Cayan, and M. D. Dettinger. 1997. "Response of Global Upper Ocean Temperature to Changing Solar Irradiance." *Journal of Geophysical Research* 102: 3255–3266. doi:10.1029/96JC03549.